Current geography masks dynamic history of gene flow during speciation in northern Australian birds

Joshua V. Peñalba[1,2,3], Leo Joseph[2,3], Craig Moritz[1,2]

Author affiliations

[1] Ecology & Evolution, Australian National University, Acton, ACT 2601, Australia

[2] Centre for Biodiversity Analysis, Acton, ACT 2601, Australia

[3] Australian National Wildlife Collection, CSIRO National Research Collections Australia, Canberra, GPO BOX 1700, Canberra, ACT 2601, Australia

Corresponding author: Joshua Penalba (josh.penalba@gmail.com)

Key words: geographic mode, allopatry, parapatry, snowballing, tipping point

Abstract

During early stages of speciation, genome divergence is greatly influenced by gene flow. As populations diverge, geography can allow or restrict gene flow in the form of barriers. Current geography, e.g. whether sister species are allopatric or parapatric, is often used to predict the potential for gene flow during the divergence process. We test the validity of this assumption in eight meliphagoid bird species codistributed across four regions. These regions are separated by known biogeographic barriers within and between northern Australia and Papua New Guinea. We find that bird populations across the same barrier have a range of divergence levels and probability of gene flow regardless of range connectivity. Geographic distance and maximum range connectivity over time can better predict divergence and probability of gene flow than whether populations are currently allopatric or parapatric. We also find support for a nonlinear decrease of the probability of gene flow during the divergence process. This implies that although gene flow influences divergence early in speciation, other factors associated with higher divergence restrict gene flow later in speciation. Current geography may then mislead inferences regarding potential for gene flow during speciation under a complex and dynamic history of geographic and reproductive isolation.

Background

Gene flow, selection, and genetic drift shape divergence during speciation, while geography sets the stage on which these forces act [1–3]. The geographic mode of speciation is defined by the extent of spatial isolation during early stages of divergence. Population pairs can have disjoint (allopatric), completely overlapping (sympatric), or separate yet partially adjoining (parapatric) ranges [4]. This geographic context predicts potential gene flow between populations. Variation in levels of gene flow affects genetic differentiation, in turn affecting the

strength of selection and drift that is necessary to drive population divergence. Alternatively, under a purely population genetic framework the geographic mode of speciation is defined by levels of gene flow; "allopatry" when the proportion of the population which are migrants (m) equals zero, "sympatry" when $m = 0.5$, and "parapatry" when $0 < m < 0.5$ per generation [5].

Although geographic and genetic definitions are often assumed to correspond, this is not always the case in nature [6]. Current range distributions between sister species are often used to infer their geographic mode of speciation, although the dynamic nature of species ranges through evolutionary time can lead to unreliable predictions of gene flow [7]. Range fluctuations during the Pleistocene's climatic cycling resulted in multiple periods of connectivity and discontinuity before resulting in the distribution we see today [8]. In order to understand how gene flow has influenced divergence during speciation, we must first understand how the geographic history could have shaped the potential for gene flow through time. The discrepancy between the spatial and population genetic definitions of the geographic mode begs the question: does current geography adequately predict realized gene flow and, consequently, divergence during early stages of speciation?

Although geographic connectivity would allow for gene flow early in speciation, later in the proces geographic connectivity can be insufficient for gene flow as populations diverge and become reproductively isolated. Populations further along in the speciation process would have reduced realized gene flow due to intrinsic incompatibilities or extrinsic selection [9]. Especially in birds, prezygotic isolation from sexual selection on song or plumage could influence gene flow in later stages of speciation. There has been growing support for the "snowball" model of accumulating incompatibility loci, initially proposed by Orr [10]. Qualitatively, this model and those derived from it specify a nonlinear accumulation of incompatibility loci resulting in a short

81 speciation duration [11]. The "snowballing" has also been modeled under scenarios with
82 moderate to no gene flow (parapatry to allopatry) meaning different geographic modes may yield
83 a similar short duration of speciation, varying only in how long it takes for speciation to initiate
84 [12–16]. This rapid accumulation of isolation has also been proposed under models of divergent
85 selection in speciation-with-gene flow and under neutral models [17–20]. Though the underlying
86 assumptions of these theories may differ, the trajectory converges to a rapid transition,
87 'snowballing', or 'tipping point' during speciation (simply referred to 'snowballing' from this
88 point forward). There is increasing empirical support for this pattern from studies of individual
89 systems [21–23] and a taxonomically broad meta-analysis [24]. More broad, comparative studies
90 across multiple systems would help elucidate this trajectory to speciation.
91 Further studies of population divergence in various geographic contexts could further
92 clarify the role of gene flow, selection and genome architecture in influencing the landscape of
93 divergence [9,20,25,26]. During speciation, local genomic variation in mutation and
94 recombination rates influence the rate at which regions diverge [25,27,28]. The geographic mode
95 of speciation could influence this landscape of divergence. Theory predicts that populations
96 diverging in parapatry should have a skewed distribution of divergence across the genome with a
97 few loci resistant to gene flow due to selection while the rest are free to move between
98 populations [29]. Populations diverging in allopatry, on the other hand, are predicted to lack this
99 skew as drift would be the predominant force influencing divergence [30,31]. This landscape
100 should also change as populations move further along the speciation continuum [9,27].
101 Here we investigate multiple bird species with populations codistributed in the same
102 region with known biogegraphic barriers. Empirical studies of gene flow during divergence in
103 relation to geography often survey closely related populations and species across different

104 geographic regions with varying biogeographic histories and selection pressures [30,31].
105 However, to understand how shifting geographic ranges can erode the correspondence between
106 current geography and realized gene flow, it is more relevant to compare a set of taxa across
107 common geography. Our study region comprises part of the monsoonal tropics of northern
108 Australia and southern Papua New Guinea containing congruent biogeographic barriers for many
109 taxa including birds [32–34]. Sea level rise since the last glacial maximum has formed a barrier
110 between northern Australia and Papua New Guinea [35]. Meanwhile, the aridification of
111 mainland Australia has resulted in multiple semipermeable terrestrial barriers with parapatrically
112 or allopatrically distributed populations. Multiple studies have shown congruent phenotypic and
113 genetic breaks for various plant and animal species in this region [34,36–39]. Here we use one
114 gerygone and seven honeyeater species co-distributed in four focal regions: Papua New Guinea
115 (PNG), Northern Territory (NT), Cape York Peninsula (CYP) and eastern Queensland (QLD)
116 that are separated by well-known barriers (figure 1). These species were chosen as they have
117 already been shown to have variation in divergence levels across known barriers between CYP
118 and QLD [40] and have varying degrees of range connectivity [41] setting the stage to compare
119 divergence in different biogeographical contexts. With this system we ask (1) how current
120 geography, or potential for gene flow, predicts realized gene flow and genome divergence during
121 early stages of speciation, (2) how genome divergence influences realized gene flow in later
122 stages of speciation, (3) and how divergence varies across different loci during the speciation
123 process. Focusing on the codistributed ranges of these species will allow us to understand how
124 the genome differentiates during speciation under different geographic contexts within and
125 between closely related systems.

126 **Methods**

Sampling

We sampled eight species with populations that occupy the four regions of interest (figure 1). For each population, we sampled three to six individuals for a total of 157 individuals (15-20 individuals per species; electronic supplementary material, table S1). Samples were chosen from locations farther away from known contact zones to avoid recent hybrids [42]. Brown honeyeater and white-throated honeyeater had insufficient sampling for PNG so only the Australian populations were used in the analyses. We extracted the DNA from all individuals using a standard salting-out procedure.

Sequencing

We sanger sequenced NADH dehydrogenase-2 (ND2) using the primers L5204 (5' TAACTAAGCTATCGGGCGCAT 3') and H6312 (5'CTTATTTAAGGCTTTGAAGGCC 3') for measures of mitochondrial divergence and structure [43]. For the nuclear loci, we used a slightly modified version of the ddRADseq protocol as described by [44]. In brief, we digested the DNA using the restriction enzymes *PstI* and *EcoRI* and size-selected 345 - 407bp. Approximately ten indexed individuals in ten pools were sequenced on a NextSeq500 for 150bp, single-read, mid-output and the rest were sequenced on another NextSeq500 lane with similar specification except with high-output. A more detailed description of lab methods is available in the electronic supplementary material.

Data processing and analyses

For each species we generated a reference set of RAD loci via the pyrad pipeline [45]. We used individuals from a different species to serve as an outgroup to polarize the SNPs in downstream analyses. Only RAD loci which have associated outgroup sequences were retained for the reference (electronic supplementary material, table S2). The resulting set of sequences

were used as a reference for further processing. Individual reads were then mapped onto this reference set using Bowtie2 (v. 2.2.2)[46]. In order to recover larger numbers of loci and avoid biases from filtering for loci with higher coverage, the mapped reads were further processed using ngsTools and ANGSD to incorporate genotype likelihood information for the various population genetic measures (v. 0.911; http://www.popgen.dk/angsd) [47].

Population structure

It has been demonstrated that more loci, even of lower coverage, yields more accurate estimates of population genetic statistics compared to fewer loci of higher coverage when using genotype likelihoods [48].We used ANGSD to further filter for SNPs to be used for downstream analyses (electronic supplementary material, table S3; see electronic supplementary material for detailed ANGSD commands). We used a minimum coverage cut-off of 2X and a maximum cut-off of 40X per individual to optimize the number of loci to be used while reducing the likelihood of recovering paralogous loci. The maximum coverage cut-off was determined by plotting a histogram of the average coverage per RAD locus and finding the upper threshold where most loci fell under. To determine population structure, we randomly chose a single SNP per RAD locus and reran ANGSD only for that set. We then used used ngsDist [49] to generate a distance matrix which we used for a principal coordinates analysis (PCoA) using 'cmdscale' from base R (v3.2.2) and a population network using SplitsTree (figure 1, electronic supplementary material figure S1) [50].

Population divergence statistics

To calculate the various population divergence statistics (F_{ST}, D_{XY}, and D_A) we used the software within the ngsTools package. These statistics were used as they provide both relative and absolute measures of genetic divergence and can be compared to previous studies [24,30,31].

We used all SNPs within each RAD locus for all per locus and global measures. To calculate pairwise F_{ST}, we used realSFS on the ANGSD genotype likelihoods to estimate an unfolded 2D site frequency spectrum (SFS) per population pair and used the SFS to derive the per locus F_{ST} estimate [51,52]. We used the same outgroups as the *pyrad* filtering steps for the unfolded SFS. To calculate global F_{ST}, we used the estimate of allele frequencies within each population and all populations pooled together $F_{ST} = H_T - H_S / H_T$ where H_T is the heterozygosity of all populations pooled and $H_S = \Sigma H_e / k$ and $H_e = 1 - \Sigma(p^2 + (1-p)^2)/m$ where k is the number of populations, m is the number of loci, and p is the allele frequency [53]. To calculate D_{XY}, we used the estimate of allele frequencies which incorporated the genotype likelihood from ANGSD [54]. To calculate D_A, we used the π estimates from ANGSD for each population and the equation $D_A = D_{XY} - (\pi_X + \pi_Y)/2$. Lastly, we used the package ape v. 4.1 to calculate the ND2 genetic p-distance under the Jukes-Cantor model [55].

Estimating the likelihood of migration

We used an approximate Bayesian computation (ABC) model selection to estimate the likelihood of migration (i.e. how strong the evidence is for some gene flow during the divergence process) between each population pair . The ABC analyses and models followed that of Roux et al. but using the unfolded 2DSFS as a summary statistic instead of the various population genetic statistics used in their study [24]. We tested the models of isolation-with-migration (IM), isolation-with-migration + heterogeneous Ne (IMhetN), isolation-with-migration + heterogeneous migration (IMhetM), isolation-with-migration + heterogeneous Ne + heterogeneous migration (IMhetNhetM), strict isolation (SI), and strict isolation + heterogeneous Ne (SIhetN). Heterogeneous Ne is modeled to reflect variation in recombination rate throughout the genome and heterogeneous migration is to reflect variation in gene flow across loci between

196 hybridizing populations. Models of SI preceding IM (secondary contact) and IM preceding SI
197 were excluded as they are typically difficult to distinguish from IM models [24]. We then used
198 the R package abc v. 2.1 and calculated the likelihood of each model using a neural network with
199 50 trained and 6 hidden networks [56]. We ran the abc analyses five times and used the average
200 model support of the replicates for further analyses. As in Roux et al., we used the sum of the
201 support for models containing a migration parameter as our probability for migration [24].
202 Additional details of the analyses can be found in the supplementary material.

203 To infer the relationship between divergence and realized gene flow, we correlated F_{ST} to
204 the probability for migration between each population pair. To negate possible circularity where
205 model support may be determined by F_{ST} itself, we calculated the F_{ST} of simulations under the SI
206 model and reran the ABC model selection on a range of F_{ST} values. If the ABC model selection
207 consistently recovers a low probability of migration, regardless of F_{ST}, high support for IM for
208 populations with lower F_{ST} in the empirical data would more likely be a biological phenomenon
209 rather than a model selection artifact.

210 *Speciation model fitting*

211 We fit our divergence versus probability of migration distribution to test support for
212 various theoretical trajectories of parapatric speciation presented by Yamaguchi and Iwasa [15].
213 The models include (1) 'threshold': where full incompatibility is reached after a certain
214 divergence level, (2) 'constant' rate of divergence increase, (3) 'accelerated' where increase in
215 divergence is small until a certain divergence threshold is reached and increase is accelerated, (4)
216 'decelerated' increase where divergence accumulates quickly but slows down as it approaches
217 full incompatibility, and (5) 'sigmoid' where the rate of increase starts slow but accelerates after
218 a certain threshold before decelerating again prior to reaching complete incompatibility

suggesting a snowballing during the speciation process (electronic supplementary material, table S4, figure S2). Our global F_{ST} parallels the 'incompatibility genetic distance' of Yamaguchi and Iwasa [15]. The inverse of our probability of migration parallels their 'incompatibility' where no support for migration ($P(m) = 0$)) is equivalent to one or full support for incompatibility ($I(z) = 1$). Identical to F_{ST} and probability of migration, the measures Yamaguchi and Iwasa used are bounded by zero and one. We used the resulting probability of migration as the summary statistic and simulated 500k distributions under each speciation trajectory model and used ABC and model rejection to estimate model support for our data. To test robustness of our ABC model inference, we used 200 simulated datasets under each model to see if the correct model is recovered (electronic supplementary material, table S5). Details regarding this method can be found in the supplementary material.

Species distribution modeling

To infer how geographic distributions have changed through time we estimated geographic connectivity over space through time using species distribution modeling and least cost path analyses. We used vouchered specimen data from the Atlas of Living Australia (http://www.ala.org.au) for occurrence points and environmental variables from WorldClim v. 1.4 (Community Climate System Model 4; http://worldclim.org/paleo-climate1) to predict species ranges under past climates. To model species distributions in R v. 3.2.2, we followed guidelines described in [57]. We used the R package dismo v. 1.1-1 for the maximum entropy (MAXENT) analyses to predict species ranges [57]. We ran MAXENT using environmental layers from the present, mid-Holocene and the LGM (electronic supplementary material, table S6). Lastly, we selected a single coordinate (midpoint of the range) for each of the four populations and calculated the geographic distance between those points to account for isolation-

by-distance. Between population pairs, we also calculated the least cost path using the R package gdistance (v. 1.1-9) based on modeled suitability [58] in the current range, mid-Holocene, and LGM predictions. For each population pair, we chose the minimum resistance path between all three time points to quantify the highest opportunity for migration through time. Habitat resistance values can be found in the electronic supplementary material table S7 and species distribution predictions can be found in figure S3.

Results

Population structure and divergence

Population structure varied between each taxon-pair though most had some form of clustering across the four populations (figure 1). Of the eight species, five showed distinct clusters for all four populations, one showed only three distinct clusters, one showed only two distinct clusters, and the last showed no population clusters (F_{ST} 0.09 - 0.39). The degrees of clustering and the population relationships are fairly variable, as shown by a PCoA and population network of the genetic distances (electronic supplementary material, figure S1). Currently allopatric populations are not more likely to be separate clusters, exemplified by samples from the PNG population often being closer to CYP and QLD. Similarly, geographically parapatric populations are not necessarily mixed as as shown by NT often being the most diverged and consistently separate cluster even for species with currently continuous geographic ranges to CYP and QLD. Mitochondrial haplotype networks generally corroborated nuclear SNP structure. Measures of genetic differentiation and divergence also varied. Autosomal and Z chromosome divergences were consistently correlated with all divergence measures (electronic supplementary material, figure S4, tables S8 and S9). Relative divergence (F_{ST}) and gene flow scales with mitochondrial divergence with a few outliers. The transition to low probability of

265 migration is fairly rapid beyond 1% ND2 p-distance. D_{XY}, an absolute measure of divergence,
266 also scales with F_{ST} but with more outliers compared to ND2 (electronic supplementary material,
267 figure S5). Though different measures of divergence in different DNA classes generally
268 correlated as expected, divergence and structure of populations varied between species with no
269 immediate patterns corresponding to geography.

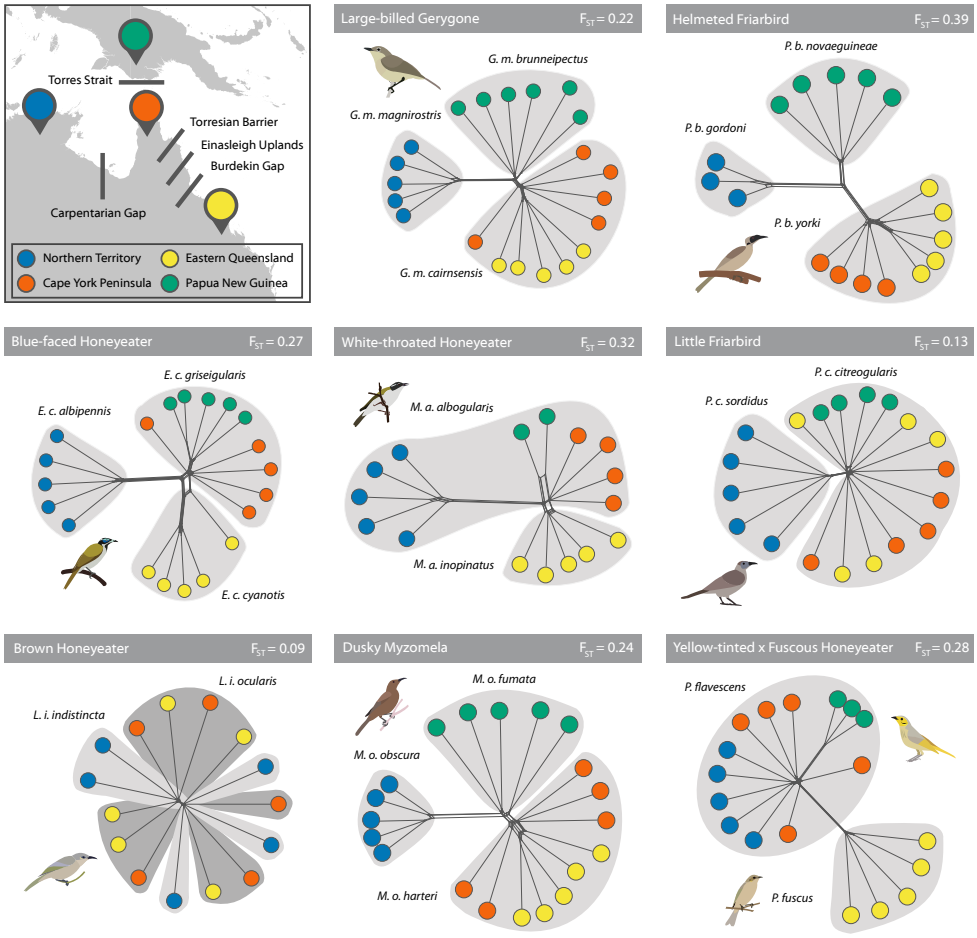

270

271 **Figure 1**. Geographic regions that were sampled for this study with corresponding known
272 biogeographical barriers. Sample networks were generated from a distance matrix estimated
273 from the ddRAD genotype likelihoods. Within each system, the species and subspecies
274 designation has been highlighted. F_{ST} represents global measures across all four populations.

275

Geography and genome divergence

Relative genome divergence (F_{ST}) and realized gene flow (probability of migration) is not predicted by between the current geographic definitions of allopatry and parapatry: allopatry between PNG and mainland Australia and either allopatry or parapatry within mainland Australia, respectively (electronic supplementary material, figure 2, figure S3, top; Kruskal-Wallis chi-squared=2.58e-03, df = 1, p = 0.9595). Population pairs exhibit a range of divergence levels regardless of whether the current barrier is terrestrial or marine. Divergence due to isolation-by-distance is well supported by a correlation between the adjusted $F_{ST}$and log of the distance in km (Spearman's rank correlation: rho = 0.427936, p = 0.004698). Correspondingly, the probability of migration also decreases with increasing distance (Spearman's rank correlation: rho = -0.482106, p = 0.001225). Lastly, we compared the minumum landscape resistance (ie. maximum range connectivity or maximum potential for gene flow corrected for distance) between the three historic time points to F_{ST} for each population pair. All comparisons with PNG had the LGM as the period where PNG was connected with north Australia (18 pairs). The timing of maximum connectivity within mainland Australia varied: eight pairs in present-day, seven during the mid-Holocene, and nine in the LGM (electronic supplementary material, table S7, figure S3). There is a positive correlation between landscape resistance and F_{ST} (Spearman's rank correlation test, S = 7048.6, rho = 0.4288, p = 0.004601), which translates to a negative correlation between resistance and probability of gene flow (Spearman's rank correlation test, S = 18102, rho = -0.466829, p = 0.00183). In sum, whereas classification of allopatry and parapatry based on predictions of current distribution do not predict divergence or probability of gene flow, other factors such as geographic distance or past connectivity proves to be more appropriate predictors.

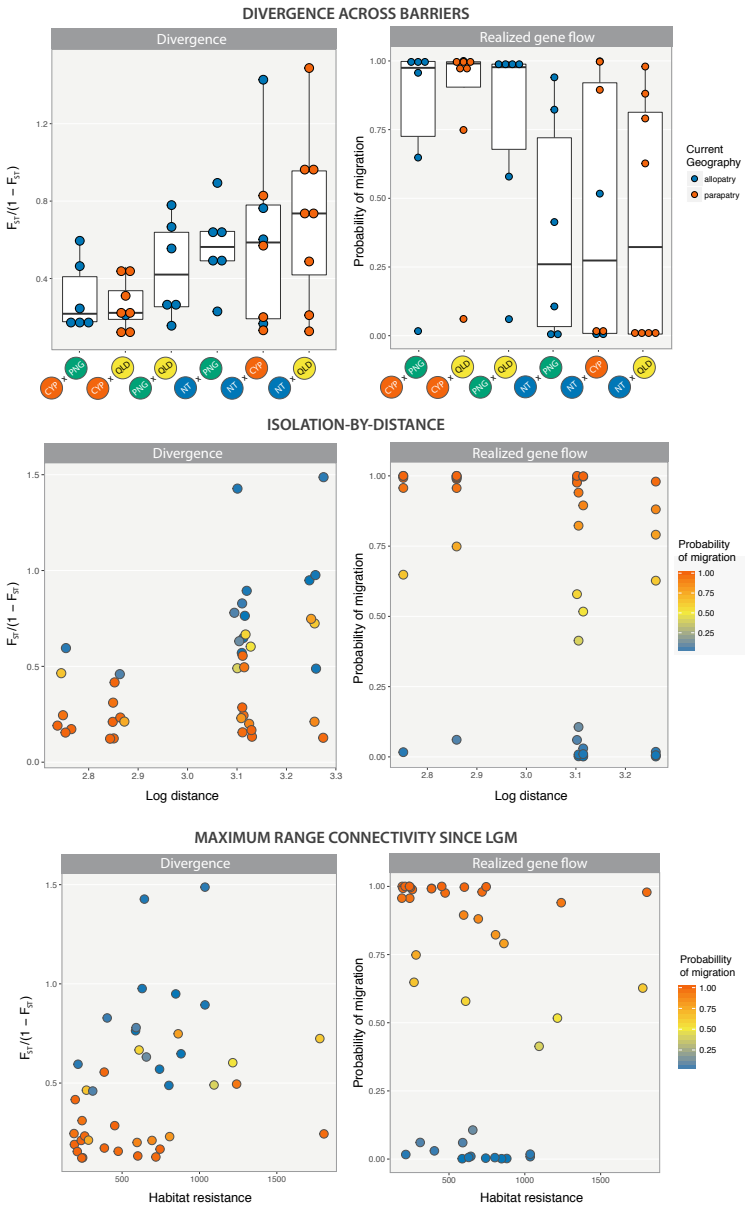

Figure 2. *Top*: Relative divergence through the barriers colored by whether or not population pairs have disjunct ranges. Allopatry and parapatry are defined based on connectivity in the species distribution models. The barriers are ordered based on increasing geographic distance *Middle*: Adjusted F_{ST} values plotted against log of distance to show isolation-by-distance. Color gradient depicts the relative support for the models with gene flow. Points have been jittered by

0.03 to display the number of points. *Bottom*: Divergence plotted against the highest connectivity across three time points (present, mid-Holocene, LGM).

Although the patterns described above also apply to the Z chromosome, the Z chromosome tends to have higher differentiation relative to the autosome. The difference between the autosomal F_{ST} value and Z chromosome Fst value increases as probability of gene flow decreases (Spearman rank correlation: rho = -0.5504, p = 1.58e-4) but does not correlate with current population connectivity (Kruskal-Wallis rank sum test: chi-squared = 0.12665, df = 1, p = 0.7219). This means that the amount of difference between autosomal and Z chromosome divergence is a function of overall divergence rather than spatial context. The difference between autosomal and Z chromosome values increases with increasing divergence for both relative (F_{ST}) and absolute divergence (D_{XY}), though absolute divergence far less so (Spearman rank correlation F_{ST}: rho = 0.715672, p = 1.001e-7; Spearman rank correlation D_{XY}: rho = 0.285595, p = 0.06674; electronic supplementary material, figure S6). In this system, broad sampling of population pairs reveal that difference between autosomal and Z chromosome divergence is likely simply related to level of divergence rather than population connectivity.

Genome divergence and speciation

Designations of allopatry or parapatry in current distributions do not predict realized gene flow, even for the less diverged populations. However, our data suggests that relative divergence level influences realized gene flow throughout the entire range of divergence. We see a rapid transition from high gene flow with low divergence to low gene flow with higher divergence through a narrow range of divergence levels; similar to the model of snowballing during speciation (figure 3). Support values for the different demographic models can be found in the

electronic supplementary material table S10. A subset of simulations under the strict isolation model was always recovered to have low probability of migration regardless of F_{ST} value, suggesting that the trajectory we see in our data is not likely due to artifacts in the model selection (figure 3).

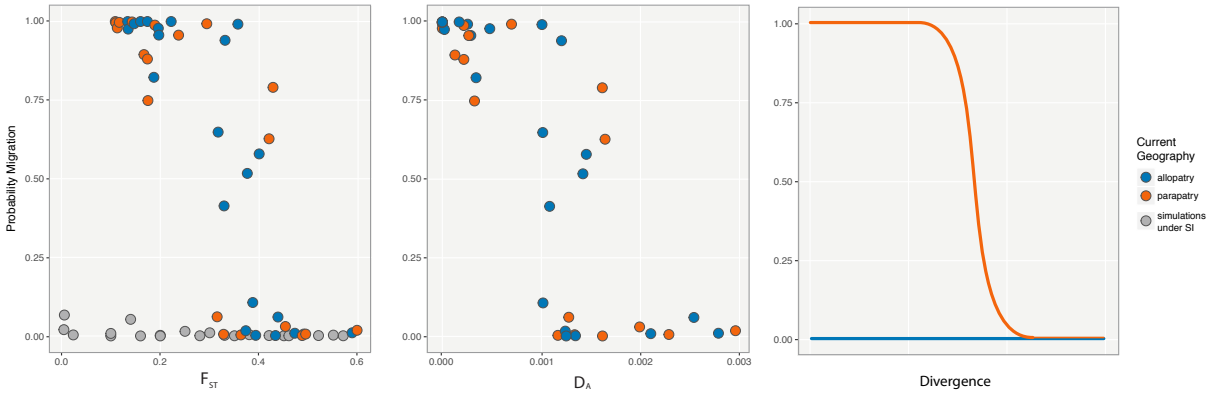

Figure 3. Probability of migration defined by the sum of ABC model supports for the 4 models with a migration parameter (IM, IMhetM, IMhetN, IMhetNhetM) plotted against F_{ST} and D_A. The third panel is a plot of our expectation of the change in probability of migration under allopatry and parapatry.

After comparing our data to models proposed by Yamaguchi and Iwasa [15], all simulations retained by the ABC model selection were those simulated under the sigmoidal function representative of a snowballing effect (electronic supplementary material, figure S2). There is no support that our data follow any other proposed trajectories. The F_{ST} range corresponding to the tipping point spans ~0.3 - 0.4. The D_A range corresponding to the tipping point is ~0.1-0.17%. Species-specific points often span the entire range of the trajectory (electronic supplementary material, figure S7). Plots for the Z chromosome, D_{XY}, and ND2 against probability of migration can be found in the electronic supplementary material, figure S8. Our system provides additional empirical support for a snowballing pattern in speciation.

Genome-wide divergence

The coefficient of variance describes the distribution of the individual F_{ST} values across the RAD loci. Higher coefficient of variance corresponds to a more skewed distribution - i.e. one in which there is higher heterogeneity in levels of divergence across loci. At lower F_{ST} values (and high gene flow) there is a lower coefficient of variance as most values are close to zero. The coefficient of variance increases with increasing F_{ST} but peaks at intermediate levels of migration and starts to decrease again when the support for migration decreases. The change in the distribution of F_{ST} values follow a predictable pattern with increasing divergence where there is an initial skew from low to moderate divergence levels followed by a more uniform distribution from moderate to high divergence levels (figure 4). This may be due to similarities in genome architecture rather than differences in current geographic classification.

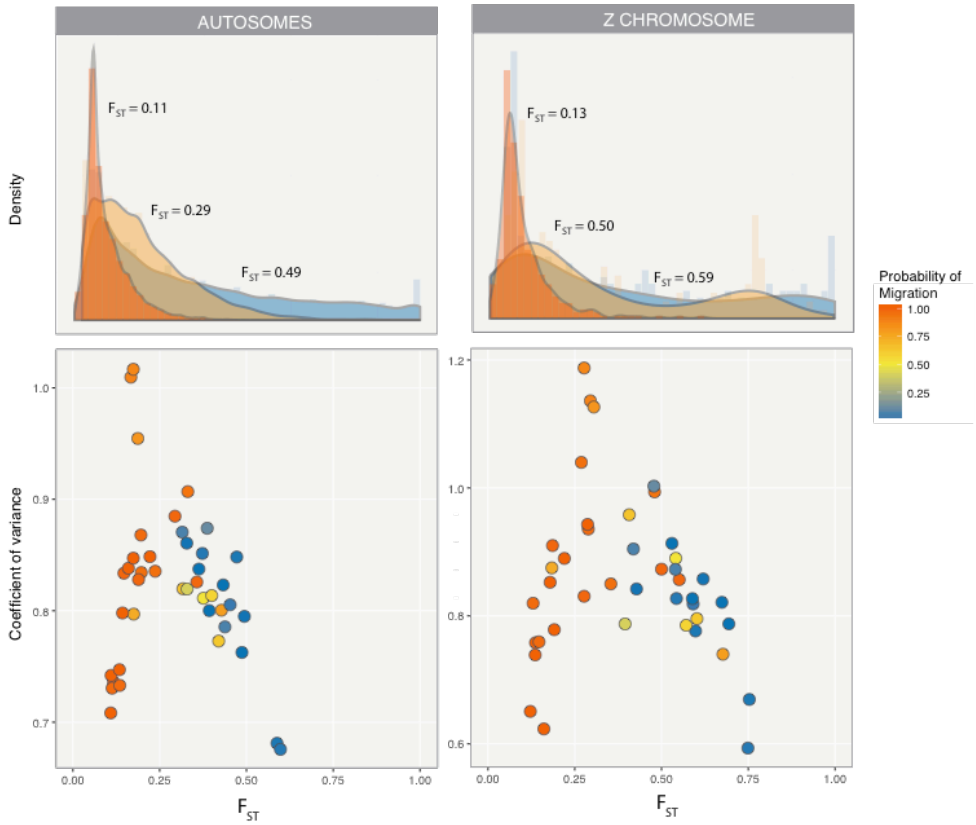

Figure 4. *Top*: Density of F_{ST} distributions of the ddRAD loci with increasing global F_{ST} and decreasing probability of migration. Three representative population pairs were chosen to represent different divergence levels. Low: Brown honeyeater NT & QLD, Medium: Blue-faced honeyeater CYP & QLD, high: White-throated honeyeater NT & QLD. *Bottom*: Distribution of the skew of F_{ST} distributions with increasing global F_{ST} and decreasing probability of migration.

Discussion

Geographic mode of speciation is expected to influence the roles of gene flow, selection, and drift on divergence. However, our data suggests that although currently continuous geographic ranges should have higher potential for gene flow relative to discontinuous ranges, it does not necessarily translate to a higher probability of migration during divergence. The degree of connectivity between populations is dynamic through their evolutionary history and this results in reticulation of the genomes between those populations (figure 1, electronic supplementary material, figure S3)[59]. Our system supports the idea that current classifications of geography (allopatric, parapatric, and sympatric) are not reflective of gene flow during population divergence [6,7]. It is possible that some currently allopatric populations have high probability of gene flow reflecting past connectivity. Conversely, some currently parapatric populations may have low probability of gene flow from incompatibilities accumulated during past allopatry. Instead, there is support for geographic distance and minumum resistance being negatively correlated with realized gene flow and positively correlated with divergence. Properly classifying the geographic mode of speciation is particularly pertinent to a dynamic region like northern Australia and PNG. Despite this correlation with distance and historical connectivity, population divergence and realized gene flow of these birds across various barriers in northern Australia and Papua New Guinea span the range of the speciation continuum potentially due to

lineage-specific biogeographic history or natural history (figure 3). Accumulating biogeographic studies across suture zones or shared biogeographical barriers show similar dynamics of population divergence in other avian systems as well as lizards and invertebrates [60–62].

Our data provides another empirical example in support for a snowballing pattern during speciation. There exists a certain threshold of divergence where there is a rapid transition between high and low gene flow likely resulting in speciation. Though populations at intermediate stages are still observed, they persist at a narrow range of divergence levels. Our data shows a similar rapid transition between the states of high and low likelihood for gene flow (figure 3). This transition occurs at a narrow stage of nuclear and mitochondrial divergence; F_{ST} ~0.3-0.4, D_A ~0.1-0.17%, and ND2 p-distances of ~1-1.5%. Using the substitution rate from Pacheco et al. (2011), the ND2 p-distances would translate to 1.11 - 1.67 Mya. The range of D_A where transition occurs is far lower to that found in Roux et al. (~0.5-2%) which may be a characteristic specific to avian speciation. Additional studies in other avian systems would help determine if these patterns in divergence are robust.

Unlike the nuclear loci, there are outliers in the mitochondrial data where populations with high mtDNA divergence would still have high likelihood of gene flow and low F_{ST} (electronic supplementry material, figure S4). These populations are from the dusky myzomela (CYP & QLD, CYP & PNG, and PNG & QLD) and from the white-throated honeyeater (CYP & QLD). The dusky myzomela population pairs are part of the small subset which are all allopatric on mainland Australia. One possible explanation for the white-throated honeyeater is that gene flow after secondary contact has homogenized the nuclear genome but maintained the local ND2 haplotypes in accordance with Haldane's rule [63].

Although neither ecological selection nor incompatibility loci were explicitly tested, this sigmoidal trajectory of speciation is consistent with the parapatric models (divergence-with-gene flow) proposed by Yamaguchi and Iwasa [15]. As suggested by the dynamic geographic history, population pairs likely experienced varying rates of gene flow through time [8,59]. On the other hand, it has also been shown that a nonlinear accumulation of divergence can occur under certain neutral scenarios [20]. Ideally, estimates of population splitting time would inform us about the timing and duration of speciation and therefore the rate of accumulating divergence; however, we found that we could not use ddRAD to infer divergence times reliably [64].

Within the genome, there is variation of divergence across loci owing to various degrees of standing genetic variation and recombination [25–27]. The change in the distribution of F_{ST} values across loci is a coarse estimate of the change in landscape of divergence through time. Although the L-shape or the skew of F_{ST} distributions between parapatrically diverging populations have been attributed to a few loci under divergent selection with the rest homogenized by gene flow [30,31], our broader sampling of population pairs show that the change in F_{ST} distribution follow a predictable pattern with increasing F_{ST} or decreasing probability of gene flow regardless of connectivity. It is also likely that this pattern of accumulation of divergence is due to variation in nucleotide diversity across the loci [20,25]. The change in skew with increasing F_{ST} could also be driven by linked selection instead of resistance to gene flow as recent studies have shown [27,65]. It would be important to complement this study with detailed studies across hybrid or suture zones to disentangle the role of gene flow and linked selection on divergence between hybridizing populations.

Finally, we note some important points for the study of the geographic mode of speciation. First, neither range overlap nor migration rate is static during speciation and it is

more likely that populations experienced various degrees of geographic connectivity and gene flow through time [59]. This is particularly pertinent for highly vagile taxa, like birds, in highly dynamic geographic regions, like the Australopapuan region. Additionally, populations that are currently allopatric due to vicariance could have experienced periods of reduced but ongoing gene flow during the formation of the barrier [66]. Second, population differentiation would also vary if a population has accumulated isolating mechanisms during allopatry and accelerated divergence during secondary contact (alloparapatry) [2]. Depending on the particular demographic history, isolation with continuous migration (primary divergence) can be difficult to distinguish from gene flow after secondary contact from genetic data alone [24]. Third, population divergence in allopatry may not necessarily translate to speciation. Seeing that most species definitions rely on degree of reproductive isolation there are no consistent criteria to differentiate discontinuous populations with no gene flow from allopatric species [1,67,68].The combination of reduced gene flow, either completely or partially, and genetic drift may result in population divergence but other factors likely play a more important role in speciation.

Conclusion

Our comparative study of divergence of bird populations through the speciation process highlights the dynamics of geographic history and their influence on divergence. Further, it provides additional support for a snowballing pattern in speciation, and it characterizes broad patterns of genomic divergence through time. The divergence that we discuss in this paper is presumed to be neutral and therefore would benefit from a replicate study looking at divergence in coding regions to observe whether different marker types have different trajectories in the same populations. The results of this broad study also clearly describe the pattern of accumulation of divergence which lend support to the emerging relevance of linked selection in

449 genome divergence. Comparative studies, particularly with multiple species in a shared
450 geographic region, help elucidate patterns of genome divergence during speciation. To fully
451 comprehend the patterns of neutral and adaptive genomic divergence, we need to sample broadly
452 both phylogenetically and geographically thus affecting shared patterns in speciation
453 differentiated from the exceptions.

454 **Author contributions**

455 JVP conceived ideas and designed the project, collected the data, performed the analyses, and led
456 the writing of the manuscript. LJ and CM provided ideas during the analysis and writing of the
457 manuscript

458 **Acknowledgments**

459 We would like to thank Ian J. Mason and Alex Drew for greatly appreciated help with collecting
460 samples in the field, Alexander Xue for assistance with demographic analyses, Matteo Fumigalli
461 for assistance with ngsTools, and Daniel Rosauer for assistance with species distribution
462 modelling. We would also like to thank Sonal Singhal, Sally Potter, and Daniel R. Wait for
463 helpful discussions and comments on the manuscript. Lastly all data collection was carried out in
464 Australian National University's Biomolecular Research Facility and most analyses were carried
465 out in the ABC Bioinformatics Development Cluster.

466 **Funding**

467 This research was funded by BirdLife Stuart Leslie Bird Research Award 2015.

468 **References**

469 1. Mayr E. 1942 *Systematics and the Origin of Species, from the Viewpoint of a Zoologist*.
470 Harvard University Press.

471 2. Coyne JA, Orr HA, Others. 2004 *Speciation*. Sinauer Associates Sunderland, MA.

472 3. White MJD. 1978 *Modes of speciation*. San Francisco: WH Freeman 455p.-Illus., maps,

chrom. nos.. General (KR, 197800185).

4. Mayr E. 1963 Animal species and evolution. *Animal species and evolution.*

5. Gavrilets S. 2003 Perspective: models of speciation: what have we learned in 40 years? *Evolution* **57**, 2197–2215.

6. Butlin RK, Galindo J, Grahame JW. 2008 Sympatric, parapatric or allopatric: the most important way to classify speciation? *Philos. Trans. R. Soc. Lond. B Biol. Sci.* **363**, 2997–3007.

7. Losos JB, Glor RE. 2003 Phylogenetic comparative methods and the geography of speciation. *Trends Ecol. Evol.* **18**, 220–227.

8. Hofreiter M, Stewart J. 2009 Ecological change, range fluctuations and population dynamics during the Pleistocene. *Curr. Biol.* **19**, R584–94.

9. Seehausen O *et al.* 2014 Genomics and the origin of species. *Nat. Rev. Genet.* **15**, 176–192.

10. Orr HA. 1995 The population genetics of speciation: the evolution of hybrid incompatibilities. *Genetics*

11. Welch JJ. 2004 Accumulating Dobzhansky-Muller incompatibilities: reconciling theory and data. *Evolution* **58**, 1145–1156.

12. Orr HA, Turelli M. 2001 The evolution of postzygotic isolation: accumulating Dobzhansky-Muller incompatibilities. *Evolution* **55**, 1085–1094.

13. Gavrilets S. 2000 Waiting time to parapatric speciation. *Proc. Biol. Sci.* **267**, 2483–2492.

14. Gavrilets S. 2014 Models of Speciation: Where Are We Now? *J. Hered.* **105**, 743–755.

15. Yamaguchi R, Iwasa Y. 2017 A tipping point in parapatric speciation. *J. Theor. Biol.* **421**, 81–92.

16. Yamaguchi R, Iwasa Y. 2013 First passage time to allopatric speciation. *Interface Focus* **3**, 20130026.

17. Via S. 2012 Divergence hitchhiking and the spread of genomic isolation during ecological speciation-with-gene-flow. *Philos. Trans. R. Soc. Lond. B Biol. Sci.* **367**, 451–460.

18. Feder JL, Egan SP, Nosil P. 2012 The genomics of speciation-with-gene-flow. *Trends Genet.* **28**, 342–350.

19. Feder JL, Nosil P, Wacholder AC, Egan SP, Berlocher SH, Flaxman SM. 2014 Genome-Wide Congealing and Rapid Transitions across the Speciation Continuum during Speciation with Gene Flow. *J. Hered.* **105**, 810–820.

20. Southcott L, Kronforst MR. In press. A neutral view of the evolving genomic architecture

of speciation. *Ecol. Evol.* (doi:10.1002/ece3.3190)

21. Matute DR, Butler IA, Turissini DA, Coyne JA. 2010 A Test of the Snowball Theory for the Rate of Evolution of Hybrid Incompatibilities. *Science* **329**, 1518–1521.

22. Moyle LC, Nakazato T. 2010 Hybrid incompatibility 'snowballs' between *Solanum* species. *Science* **329**, 1521–1523.

23. Riesch R *et al.* 2017 Transitions between phases of genomic differentiation during stick-insect speciation. *Nature Ecology & Evolution* **1**, 0082.

24. Roux C, Fraïsse C, Romiguier J, Anciaux Y, Galtier N, Bierne N. 2016 Shedding Light on the Grey Zone of Speciation along a Continuum of Genomic Divergence. *PLoS Biol.* **14**, e2000234.

25. Cruickshank TE, Hahn MW. 2014 Reanalysis suggests that genomic islands of speciation are due to reduced diversity, not reduced gene flow. *Mol. Ecol.* **23**, 3133–3157.

26. Ravinet M, Faria R, Butlin RK, Galindo J, Bierne N, Rafajlović M, Noor MAF, Mehlig B, Westram AM. 2017 Interpreting the genomic landscape of speciation: a road map for finding barriers to gene flow. *J. Evol. Biol.* **30**, 1450–1477.

27. Burri R *et al.* 2015 Linked selection and recombination rate variation drive the evolution of the genomic landscape of differentiation across the speciation continuum of Ficedula flycatchers. *Genome Res.* **25**, 1656–1665.

28. Ellegren H *et al.* 2012 The genomic landscape of species divergence in *Ficedula* flycatchers. *Nature* **491**, 756–760.

29. Martinsen GD, Whitham TG, Turek RJ, Keim P. 2001 Hybrid populations selectively filter gene introgression between species. *Evolution* **55**, 1325–1335.

30. Martin SH *et al.* 2013 Genome-wide evidence for speciation with gene flow in Heliconius butterflies. *Genome Res.* (doi:10.1101/gr.159426.113)

31. Nosil P, Gompert Z, Farkas TE, Comeault AA, Feder JL, Buerkle CA, Parchman TL. 2012 Genomic consequences of multiple speciation processes in a stick insect. *Proc. Biol. Sci.* **279**, 5058–5065.

32. Edwards RD, Crisp MD, Cook DH, Cook LG. 2017 Congruent biogeographical disjunctions at a continent-wide scale: Quantifying and clarifying the role of biogeographic barriers in the Australian tropics. *PLoS One* **12**, e0174812.

33. Cracraft J. 1986 Origin and evolution of continental biotas: speciation and historical congurence within the Australian avifauna. *Evolution* **40**, 977–996.

34. Bowman DMJS *et al.* 2010 Biogeography of the Australian monsoon tropics. *J. Biogeogr.* **37**, 201–216.

539 35. Lambeck K, Chappell J. 2001 Sea Level Change Through the Last Glacial Cycle. *Science*
540 **292**, 679–686.

541 36. Baldassarre DT, White TA, Karubian J, Webster MS. 2014 Genomic and morphological
542 analysis of a semipermeable avian hybrid zone suggests asymmetrical introgression of a
543 sexual signal. *Evolution* **68**, 2644–2657.

544 37. Catullo RA, Lanfear R, Doughty P, Keogh JS. 2014 The biogeographical boundaries of
545 northern Australia: evidence from ecological niche models and a multi-locus phylogeny of
546 Uperoleia toadlets (Anura: Myobatrachidae). *J. Biogeogr.* **41**, 659–672.

547 38. Edwards SV, Potter S, Schmitt CJ. 2016 Reticulation, divergence, and the phylogeography–
548 phylogenetics continuum. *Proceedings of the*

549 39. Kearns AM, Joseph L, Omland KE, Cook LG. 2011 Testing the effect of transient Plio-
550 Pleistocene barriers in monsoonal Australo-Papua: did mangrove habitats maintain genetic
551 connectivity in the Black Butcherbird? *Mol. Ecol.* **20**, 5042–5059.

552 40. Peñalba JV, Mason IJ, Schodde R, Moritz C, Joseph L. In press. Characterizing divergence
553 through three adjacent Australian avian transition zones. *J. Biogeogr.*
554 (doi:10.1111/jbi.13048)

555 41. R. Schodde, Mason IJ. 1999 The Directory of Australian Birds. Passerines. CSIRO
556 Publishing: Melbourne

557 42. Ford J. 1987 Hybrid Zones in Australian Birds. *Emu* **87**, 158–178.

558 43. Sorenson MD, Ast JC, Dimcheff DE, Yuri T, Mindell DP. 1999 Primers for a PCR-based
559 approach to mitochondrial genome sequencing in birds and other vertebrates. *Mol.*
560 *Phylogenet. Evol.* **12**, 105–114.

561 44. Peterson BK, Weber JN, Kay EH, Fisher HS, Hoekstra HE. 2012 Double digest RADseq:
562 an inexpensive method for de novo SNP discovery and genotyping in model and non-model
563 species. *PLoS One* **7**, e37135.

564 45. Eaton DAR. 2014 PyRAD: assembly of de novo RADseq loci for phylogenetic analyses.
565 *Bioinformatics* **30**, 1844–1849.

566 46. Langmead B, Salzberg SL. 2012 Fast gapped-read alignment with Bowtie 2. *Nat. Methods*
567 **9**, 357–359.

568 47. Korneliussen TS, Albrechtsen A, Nielsen R. 2014 ANGSD: Analysis of Next Generation
569 Sequencing Data. *BMC Bioinformatics* **15**, 356.

570 48. Fumagalli M, Vieira FG, Korneliussen TS, Linderoth T, Huerta-Sánchez E, Albrechtsen A,
571 Nielsen R. 2013 Quantifying population genetic differentiation from next-generation
572 sequencing data. *Genetics* **195**, 979–992.

573 49. Vieira FG, Lassalle F, Korneliussen TS, Fumagalli M. 2016 Improving the estimation of
574 genetic distances from Next-Generation Sequencing data. *Biol. J. Linn. Soc. Lond.* **117**,
575 139–149.

576 50. Huson DH. 1998 SplitsTree: analyzing and visualizing evolutionary data. *Bioinformatics*
577 **14**, 68–73.

578 51. Reynolds J, Weir BS, Cockerham CC. 1983 Estimation of the coancestry coefficient: basis
579 for a short-term genetic distance. *Genetics* **105**, 767–779.

580 52. Weir BS, Cockerham CC. 1984 ESTIMATING F-STATISTICS FOR THE ANALYSIS OF
581 POPULATION STRUCTURE. *Evolution* **38**, 1358–1370.

582 53. Hartl DL, Clark AG, Clark AG. 1997 *Principles of population genetics*. Sinauer associates
583 Sunderland.

584 54. Korneliussen TS, Moltke I, Albrechtsen A, Nielsen R. 2013 Calculation of Tajima's D and
585 other neutrality test statistics from low depth next-generation sequencing data. *BMC*
586 *Bioinformatics* **14**, 289.

587 55. Paradis E, Claude J, Strimmer K. 2004 APE: Analyses of Phylogenetics and Evolution in R
588 language. *Bioinformatics* **20**, 289–290.

589 56. Csilléry K, François O, Blum MGB. 2012 abc: an R package for approximate Bayesian
590 computation (ABC). *Methods Ecol. Evol.* **3**, 475–479.

591 57. Hijmans RJ, Elith J. 2013 Species distribution modeling with R. *R package version 0. 8-11*

592 58. van Etten J. 2017 R Package gdistance: Distances and Routes on Geographical Grids.
593 *Journal of Statistical Software, Articles* **76**, 1–21.

594 59. Rheindt FE, Edwards SV. 2011 Genetic introgression: an integral but neglected component
595 of speciation in birds. *Auk* **128**, 620-632

596 60. Singhal S, Bi K. 2017 History cleans up messes: the impact of time in driving divergence
597 and introgression in a tropical suture zone. *Evolution* (doi:10.1111/evo.13278)

598 61. Winger BM, Bates JM. 2015 The tempo of trait divergence in geographic isolation: avian
599 speciation across the Marañon Valley of Peru. *Evolution* **69**, 772–787.

600 62. Whinnett A, Zimmermann M, Willmott KR, Herrera N, Mallarino R, Simpson F, Joron M,
601 Lamas G, Mallet J. 2005 Strikingly variable divergence times inferred across an Amazonian
602 butterfly 'suture zone'. *Proc. Biol. Sci.* **272**, 2525–2533.

603 63. Price TD, Bouvier MM. 2002 The evolution of F1 postzygotic incompatibilities in birds.
604 *Evolution* **56**, 2083–2089.

605 64. Shafer ABA, Peart CR, Tusso S, Maayan I, Brelsford A, Wheat CW, Wolf JBW. 2016

606 Bioinformatic processing of RAD-seq data dramatically impacts downstream population
607 genetic inference. *Methods Ecol. Evol.* (doi:10.1111/2041-210X.12700)

608 65. Wang J, Street NR, Scofield DG, Ingvarsson PK. 2016 Variation in Linked Selection and
609 Recombination Drive Genomic Divergence during Allopatric Speciation of European and
610 American Aspens. *Mol. Biol. Evol.* **33**, 1754–1767.

611 66. Yang M, He Z, Shi S, Wu C-I. 2017 Can genomic data alone tell us whether speciation
612 happened with gene flow? *Mol. Ecol.* **26**, 2845–2849.

613 67. Harvey MG, Seeholzer GF, Smith BT, Rabosky DL, Cuervo AM, Brumfield RT. 2017
614 Positive association between population genetic differentiation and speciation rates in New
615 World birds. *Proc. Natl. Acad. Sci. U. S. A.* (doi:10.1073/pnas.1617397114)

616 68. Sukumaran J, Knowles LL. 2017 Multispecies coalescent delimits structure, not species.
617 *Proc. Natl. Acad. Sci. U. S. A.* **114**, 1607–1612.